ANALYTICAL CALCULATION OF TRANSVERSE EMITTANCE AND TWISS PARAMETERS

S. Marini, L. Batista, N. Chauvin, A. Chancé, D. Uriot, P. A. P. Nghiem
CEA, Université Paris-Saclay, Gif-sur-Yvette, France

Abstract

Achieving plasma-based accelerators for users demands careful control not only of the beam energy and energy spread, but also of transverse beam properties such as emittance, size, and divergence. Since plasma-based accelerators typically produce beams with significantly larger energy spread and emittance than conventional RF accelerators, several questions remain to be addressed, particularly, the transverse beam dynamics. In this article, it is presented an analytical description of the transverse beam properties evolution in a constant-focusing channel representing a plasma density plateau assuming a finite energy spread. The resulting expressions provide qualitative and quantitative guide to understand the transverse beam dynamics under these conditions.

INTRODUCTION

Laser-plasma accelerators are moving from proof-of-principle experiments to a realistic option for compact accelerator facilities [1, 2]. Their main advantage is the accelerating gradient, which can reach 10–100 GV/m, making it possible to reduce typical machine length by orders of magnitude. Recent laser-plasma accelerator studies report strong beam quality at the plasma exit [3–8]. The main challenge is now make stable and repeatable the beam delivery at the user point, where transverse beam quality is critical.

Achieving operational plasma-based accelerators requires integrated studies to control not only the beam energy and energy spread, but also of transverse beam properties such as emittance, size, and divergence. The transverse beam dynamics is governed by the focusing gradient K. In a plasma density plateau, K is typically of order 10^6 m^{-2}, whereas in the surrounding magnetic transport lines the effective focusing is only a few m^{-2}. In presence of energy spread, such large variations of K across interfaces are the main reason of beam Twiss mismatch and consequent emittance growth [9–11].

To qualify and quantify the transverse beam properties evolution, particularly the emittance, we present a fully analytical description for a constant-focusing channel representing a plasma density plateau acting over an electron beam with finite energy spread.

The work described in this article expands the model presented in Ref. [11] in contrast to earlier works [10] (semi-analytical) calculation, the energy spread is here kept up to second order. Then, an analytical expression of emittance growth in a constant-K channel with finite energy spread is derived, from which the Twiss-parameter evolution, the decoherence length, and the saturated emittance are obtained.

THE KEY PARAMETER K

The plasma wakefield focuses particles in all the transverse planes. It can be considered as a cylindrically symmetric focusing channel, characterized by the focusing gradient K (in m^{-2}) expressed as

$$K = \frac{e}{\gamma_{\mathrm{rel}} m_e c^2} \left(\frac{\partial E_r}{\partial r} - \beta_{\mathrm{rel}} c \frac{\partial B_\theta}{\partial r} \right)\Big|_{r=0}, \tag{1}$$

where e and m_e are the electron charge and mass, c is the speed of light in vacuum, β_{rel} and γ_{rel} are the relativistic speed and Lorentz factor, r the transverse coordinate and E_r, B_θ the radial electric and azimutal magnetic field components.

Because K depends explicitly on the beam energy through γ_{rel}, the focusing is chromatic. For a particle with momentum deviation $\delta = \Delta p/p_0$, the effective focusing gradient becomes

$$K^* \equiv \frac{K}{1+\delta}, \tag{2}$$

where K is the focusing gradient defined in Eq. (1) for the reference particle, which has $\delta = 0$ and Lorentz factor γ_{rel}. Particles with different energies are focused differently, inducing oscillations on the beta functions, which in turn induce emittance growth by the phase mixing mechanism. All these will be explicitly derived in the following.

EVOLUTION OF THE TWISS PARAMETERS

To model the plasma-density plateau, we assume that the focusing gradient K remains constant along the propagation direction. The transverse coordinate u ($u = x$ or y) of a particle then follows Hill's equation

$$u'' + K^* u = 0, \tag{3}$$

whose general solution is given by

$$u = u_0 \cos[z\sqrt{K^*}] + \frac{u_0'}{\sqrt{K^*}} \sin[z\sqrt{K^*}], \tag{4}$$

$$u' = -u_0\sqrt{K^*} \sin[z\sqrt{K^*}] + u_0' \cos[z\sqrt{K^*}]. \tag{5}$$

The projected transverse emittance of the beam is defined from the second-order moments as

$$\varepsilon^2 = \langle u^2 \rangle \langle u'^2 \rangle - \langle uu' \rangle^2. \tag{6}$$

These moments can be written in terms of the Twiss parameters according to

$$\langle u^2 \rangle = \beta\varepsilon, \qquad \langle u'^2 \rangle = \gamma\varepsilon, \qquad \langle uu' \rangle = -\alpha\varepsilon, \tag{7}$$

where $\langle\cdot\rangle$ denotes an average over the particle distribution $\Psi(u,u',\delta)$. Thus, $\langle u^2\rangle$, $\langle u'^2\rangle$, and $\langle uu'\rangle$ are the beam-size, divergence, and phase-space correlation moments, respectively. The quantities α, β, and γ are the Twiss parameters. Assuming no correlation between the transverse coordinates (u,u') and the energy deviation δ, the distribution factorizes as $\Psi(u,u',\delta) = g(u,u')f(\delta)$, and the average of a quantity χ becomes

$$\langle\chi\rangle = \int\Big[\iint \chi g\,(u,u')\,dudu'\Big]f(\delta)d\delta. \tag{8}$$

The double integral over (u,u') can be evaluated by expressing the second-order moments $\langle u_0^2\rangle$, $\langle u_0'^2\rangle$, and $\langle u_0u_0'\rangle$ in terms of the entrance Twiss parameters, resulting for instance, in the position variance:

$$\frac{\langle u^2\rangle}{\varepsilon_0} = \int\Big[\beta_0\cos^2(z\sqrt{K^*}) - 2\alpha_0\frac{\cos(z\sqrt{K^*})\sin(z\sqrt{K^*})}{\sqrt{K^*}} + \frac{\gamma_0}{K^*}\sin^2(z\sqrt{K^*})\Big]f(\delta)d\delta. \tag{9}$$

We assume δ follows a Gaussian distribution with rms width σ_δ, uncorrelated with (u,u'), so:

$$f(\delta) = \frac{1}{\sqrt{2\pi}\sigma_\delta}\exp\left(\frac{-\delta^2}{2\sigma_\delta^2}\right). \tag{10}$$

For $|\delta|\ll 1$, we expand $K^* = K^*(\delta)$ and the trigonometric arguments in Eq. (9) to $\mathcal{O}(\delta^2)$ before performing the energy average by solving the integral. To expand $\cos^2(z\sqrt{K^*})$ with $|\delta|\ll 1$, for example, we note that:

$$\cos^2\Big(z\sqrt{\tfrac{K}{1+\delta}}\Big) = \frac{1}{2} + \frac{1}{2}\cos\Big(2z\sqrt{\tfrac{K}{1+\delta}}\Big),$$

where the phase argument can be expanded in powers of δ as

$$2z\sqrt{\frac{K}{1+\delta}} = 2z\sqrt{K}\left(1 - \frac{\delta}{2} + \frac{3}{8}\delta^2 - \cdots\right).$$

From the identity $\cos(a+b) = \cos a\cos b - \sin a\sin b$, with $a = 2z\sqrt{K}(1-\delta/2)$ and $b = (3/4)z\sqrt{K}\delta^2$, we expand and observe the terms proportional to δ^2 reads $\cos\left(3z\sqrt{K}\delta^2/4\right) \approx 1$ and $\sin\left(3z\sqrt{K}\delta^2/4\right) \approx 3z\sqrt{K}\delta^2/4$. Putting it together:

$$\cos^2\Big(z\sqrt{\tfrac{K}{1+\delta}}\Big) \approx \tfrac{1}{2} + \tfrac{1}{2}\cos\Big(2z\sqrt{K}(1-\tfrac{\delta}{2})\Big) - \tfrac{3}{8}z\sqrt{K}\,\delta^2\,\sin\Big(2z\sqrt{K}(1-\tfrac{\delta}{2})\Big), \tag{11}$$

and analogously for $\sin^2$ and mixed products. The Gaussian average is then reduced to integrals of the form $\int d\delta\,\cos(\phi_0 - c\delta)\,e^{-\delta^2/2\sigma_\delta^2} \propto \cos(\phi_0)\,e^{-c^2\sigma_\delta^2/2}$, with c, here proportional to $z\sqrt{K}$. Also, integrals proportional to δ^2 appear and their solution are obtained directly by differentiation with respect to c, such as $\partial_c^2\int d\delta\,\cos(\phi_0 - c\delta)\,e^{-\delta^2/2\sigma_\delta^2} \propto -\cos(\phi_0)\,\sigma_\delta^2\left(1-c^2\sigma_\delta^2\right)e^{-c^2\sigma_\delta^2/2}$, and similarly for the sine terms.

After averaging over δ, the second moments read:

$$\frac{\langle u^2\rangle}{\varepsilon_0} = \frac{b_+}{\sqrt{K}} - \frac{e^{-\frac{1}{2}\sigma_\delta^2 z^2K}}{\sqrt{K}}\Big[\Big(\alpha_0 - \frac{\sigma_\delta^2}{8}(\alpha_0 - 3zK\beta_0 - z\gamma_0)\Big)\sin(2z\sqrt{K}) + \Big(b_- + \frac{\sigma_\delta^2}{4}z\sqrt{K}\,\alpha_0\Big)\cos(2z\sqrt{K})\Big], \tag{12}$$

$$\frac{\langle u'^2\rangle}{\varepsilon_0} = \sqrt{K}\,b_+ + \sigma_\delta^2\frac{K\beta_0}{2} + \sqrt{K}\,e^{-\frac{1}{2}\sigma_\delta^2 z^2K}\Big[\Big(\alpha_0 + \frac{\sigma_\delta^2}{8}(3\alpha_0 + 7zK\beta_0 - 3z\gamma_0)\Big)\sin(2z\sqrt{K}) + \Big(b_- + \frac{\sigma_\delta^2}{4}\sqrt{K}(5z\alpha_0 - 2\beta_0)\Big)\cos(2z\sqrt{K})\Big], \tag{13}$$

$$\frac{\langle u\,u'\rangle}{\varepsilon_0} = e^{-\frac{1}{2}\sigma_\delta^2 z^2K}\Big[\Big(b_- + \frac{\sigma_\delta^2}{16\sqrt{K}}(12zK\alpha_0 - 3K\beta_0 - \gamma_0)\Big)\sin(2z\sqrt{K}) - \Big(\alpha_0 + \frac{\sigma_\delta^2}{8}z(5K\beta_0 - \gamma_0)\Big)\cos(2z\sqrt{K})\Big], \tag{14}$$

with

$$b_\pm \equiv \frac{\gamma_0}{2\sqrt{K}} \pm \frac{\beta_0\sqrt{K}}{2} \tag{15}$$

the dimensionless mismatch parameters. Note that, the second moments in Eq. (7), together with Eqs. (12)–(14), describe the evolution of the Twiss parameters once the emittance is specified. For $\alpha_0 = 0$ and $\beta_0 = 1/\sqrt{K}$, one has $b_+ = 1$ and $b_- = 0$. Then, in the limit of small energy spread, $\sigma_\delta^2 \to 0$, all oscillatory terms in Eqs. (12)–(14) vanish, and one recovers the so-called matched injection condition, where the Twiss parameter β and the rms beam size remain constant throughout the focusing channel.

EMITTANCE GROWTH

Substituting Eqs. (12)–(14) into (6) and retaining terms to order σ_δ^2 yields the emittance evolution:

$$\frac{\varepsilon^2(z)}{\varepsilon_0^2} = b_+^2 + \sigma_\delta^2\frac{\sqrt{K}\beta_0}{2}\,b_+ + e^{-\sigma_\delta^2 z^2K}(1-b_+^2) - \frac{\sigma_\delta^2}{8}\,e^{-\sigma_\delta^2 z^2K}\Big[\alpha_0^2 + 8z\sqrt{K}\,\alpha_0 b_+ - (3\sqrt{K}\beta_0 + b_+)b_- + 2\alpha_0 b_-\sin(4z\sqrt{K}) - (\alpha_0^2 - b_-^2)\cos(4z\sqrt{K})\Big] + \frac{\sigma_\delta^2}{2}\,e^{-\frac{1}{2}\sigma_\delta^2 z^2K}\Big[(-\beta_0\gamma_0 + 2z\sqrt{K}\,\alpha_0 b_+)\cos(2z\sqrt{K}) + b_-(\alpha_0 - 2z\sqrt{K}\,b_+)\sin(2z\sqrt{K})\Big]. \tag{16}$$

Several properties follow directly from Eq. (16). For a monoenergetic beam ($\sigma_\delta = 0$), then $\varepsilon^2/\varepsilon_0^2 = 1$, and the beam phase-space area is preserved.

For $\sigma_\delta > 0$, Eq. (16) shows that the emittance oscillates while growing, driven by phase mixing between energy slices. Entrance mismatch, quantified by α_0 and β_0, sets the amplitude of betatron oscillations (wavenumbers $2\sqrt{K}$ and $4\sqrt{K}$) as the characteristic ellipses associated with different energy slices rotate at different rates in (u, u'). These oscillations are progressively damped by the Gaussian factors $e^{-\sigma_\delta^2 K z^2/2}$ and $e^{-\sigma_\delta^2 K z^2}$, and the emittance approaches a saturated value once the oscillatory contributions are fully damped. The damping rate scales as $\sigma_\delta\sqrt{K}$, while the growth amplitude is set by the entrance mismatch.

In summary, when the Twiss parameters of the injected beam are mismatched, each beam energy slice oscillates in phase space with different frequencies. This leads to an increase in the projected phase-space area, and then in the emittance, until a saturated value is reached.

DECOHERENCE LENGTH AND SATURATED EMITTANCE

We estimate the decoherence length z_D as the propagation distance at which oscillation in the emittance value decays to a residual fraction $r_d \in (0, 1)$ of its initial amplitude.

The oscillatory part of the emittance evolution in Eq. (16) is damped by Gaussian factors of the form $\exp\left(-\sigma_\delta^2 K z^2/\mathscr{C}\right)$, with $\mathscr{C} = 1$ or 2. Defining the decoherence length z_D as the distance over which the amplitude of the emittance oscillations decreases to a fraction r_d of its initial value yields

$$z_D = \frac{\sqrt{\mathscr{C}\ln(1/r_d)}}{\sigma_\delta\sqrt{K}}. \tag{17}$$

For $r_d = 1\%$, the prefactor $\sqrt{\mathscr{C}\ln(1/r_d)}$ is approximately 2.15 when $\mathscr{C} = 1$ and 3.0 when $\mathscr{C} = 2$. Equation (16) further shows that the dominant damping term depends on the injection conditions: the term with $\mathscr{C} = 2$ dominates for a matched beam, and also for an unmatched beam with large energy spread, whereas the term with $\mathscr{C} = 1$ dominates for an unmatched beam with small energy spread.

For $z \gg z_D$ (*i.e.*, $z \to \infty$), the emittance reaches saturation at:

$$\frac{\varepsilon_{\rm sat}}{\varepsilon_0} = \sqrt{b_+^2 + \sigma_\delta^2\frac{\sqrt{K}\beta_0}{2}}\, b_+. \tag{18}$$

For small energy spread ($\sigma_\delta^2 \ll 1$) and considering the beam Twiss parameters at the entrance, it simplifies to:

$$\frac{\varepsilon_{\rm sat}}{\varepsilon_0} \approx \left(\frac{1+\alpha_0^2}{2\beta_0\sqrt{K}} + \frac{\beta_0\sqrt{K}}{2}\right) + \sigma_\delta^2\frac{\beta_0\sqrt{K}}{4}. \tag{19}$$

Equation (18) shows that the saturated emittance value is set primarily by the entrance mismatch through b_+, while the focusing gradient and the energy spread controls the decoherence length z_D. For matched injection the residual growth reduces to $\varepsilon_{\rm sat}/\varepsilon_0 \approx 1 + \sigma_\delta^2/4$, a small purely chromatic contribution of second order in σ_δ.

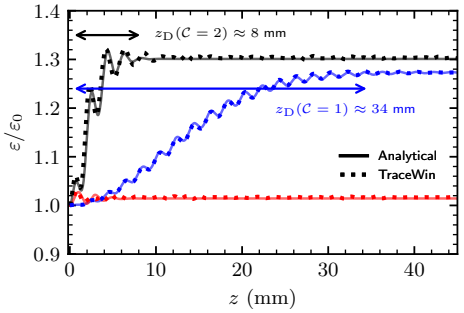

Figure 1: Evolution of the normalized emittance through a constant focusing plasma density plateau, obtained from analytical (solid lines) and TraceWin (dotted lines) calculations. Results are shown for the unmatched (α_u, β_u) case with $\sigma_\delta = 4\%$ (blue) and 24% (black), and for the matched case (α_m, β_m) with $\sigma_\delta = 24\%$ (red).

In Fig. 1, we compare the analytical emittance evolution with numerical simulations performed with the tracking code TraceWin [12] for a 200 MeV electron beam with negligible charge and a longitudinal size of 3 µm, propagating under a constant focusing gradient $K = 2.48 \times 10^6\ \mathrm{m}^{-2}$. In TraceWin, the transverse dynamics is reproduced using dedicated plasma-equivalent focusing elements, *plasmaquad* (also referred as *quadspec* [13]), while the longitudinal dynamics is left unchanged. As a result, the energy and energy spread remains constant throughout the plasma, consistent with the presented analytical assumptions. We also consider a low-charge beam such that collective effects can be neglected. For matched injection conditions, $\alpha_0 = \alpha_m$ and $\beta_0 = \beta_m$, a very small but finite emittance growth is still visible, in agreement with Eq. (19). For unmatched cases, $\alpha_0 = \alpha_u = 0.3$ and $\beta_0 = \beta_u = 2\beta_m$, oscillations are observed, followed by saturation at the corresponding decoherence length z_D consistent with Eq. (17). Overall, the analytical predictions are in excellent agreement with the numerical results, which supports the present analysis.

CONCLUSION

An analytical expression for the emittance growth in a constant-focusing channel has been derived to second order in σ_δ, built according the analytical model introduced in Ref. [11], where the case of varying K is also studied. The results describe the oscillations of the Twiss parameters, their progressive damping by phase mixing, and the associated emittance increase up to saturation. The characteristic length scale for this process is the decoherence length $z_D \propto (\sigma_\delta\sqrt{K})^{-1}$, while the saturated emittance is set mainly by the entrance Twiss parameters mismatch through (α_0, β_0), with a weak second-order dependence on σ_δ. The model assumes a second-order expansion in energy spread, and no correlation between the longitudinal and transversal beam dynamics. In these limits, it provides a reference for numerical tracking and a practical guide for beam matching studies in plasma cells.

REFERENCES

[1] T. Tajima and J. M. Dawson, "Laser Electron Accelerator", *Phys. Rev. Lett.*, vol. 43, no. 4, p. 267, Jul. 1979. doi:10.1103/PhysRevLett.43.267

[2] E. Esarey, C. B. Schroeder, and W. P. Leemans, "Physics of laser-driven plasma-based electron accelerators", *Rev. Mod. Phys.*, vol. 81, no. 3, p. 1229, Aug. 2009. doi:10.1103/RevModPhys.81.1229

[3] M. Kirchen *et al.*, "Optimal beam loading in a laser-plasma accelerator", *Phys. Rev. Lett.*, vol. 126, no. 17, p. 174801, Apr. 2021. doi:10.1103/PhysRevLett.126.174801

[4] L. T. Dickson *et al.*, "Mechanisms to control laser-plasma coupling in laser wakefield accelerators", *Phys. Rev. Accel. Beams*, vol. 25, no. 10, p. 101301, Oct. 2022. doi:10.1103/PhysRevAccelBeams.25.101301

[5] P. Drobniak *et al.*, "Random scan optimization of a laser-plasma electron injector based on fast particle-in-cell simulations", *Phys. Rev. Accel. Beams*, vol. 26, no. 9, p. 091302, Sep. 2023. doi:10.1103/PhysRevAccelBeams.26.091302

[6] P. Drobniak *et al.*, "Validation of a compact and tunable continuous gas-flow laser-plasma target for electron beam production above 150 MeV", *Appl. Sci.*, vol. 16, no. 5, p. 2312, Mar. 2026. doi:10.3390/app16052312

[7] S. Marini *et al.*, "Beam physics studies for a high charge and high beam quality laser-plasma accelerator", *Phys. Rev. Accel. Beams*, vol. 27, no. 6, p. 063401, Jun. 2024. doi:10.1103/PhysRevAccelBeams.27.063401

[8] T. L. Steyn *et al.*, "Observation of laser plasma accelerated electrons with transverse momentum spread below the thermal level", Jun. 2025, arXiv:2506.18047 [physics.plasm-ph]. doi:10.48550/arXiv.2506.18047

[9] T. J. Mehrling, J. Grebenyuk, F. S. Tsung, K. Floettmann, and J. Osterhoff, "Transverse emittance growth in staged laser-wakefield acceleration", *Phys. Rev. ST Accel. Beams*, vol. 15, no. 11, p. 111303, Nov. 2012. doi:10.1103/PhysRevSTAB.15.111303

[10] A. Aschikhin, T. J. Mehrling, A. Martinez de la Ossa, and J. Osterhoff, "Analytical model for the uncorrelated emittance evolution of externally injected beams in plasma-based accelerators", *Nucl. Instrum. Methods Phys. Res. A*, vol. 909, p. 414, Nov. 2018. doi:10.1016/j.nima.2018.02.065

[11] L. Batista, S. Marini, N. Chauvin, A. Chancé, D. Uriot, and P. A. P. Nghiem, "Beam transverse dynamics in laser-plasma accelerators", *Phys. Rev. E*, vol. 113, no. 4, p. 045207, Apr. 2026. doi:10.1103/6g4s-8d81

[12] D. Uriot and N. Pichoff, "Status of TraceWin code", in *Proc. 6th Int. Particle Accelerator Conf. (IPAC'15)*, Richmond, VA, USA, May 2015, p. 92. doi:10.18429/JACoW-IPAC2015-MOPWA008

[13] L. Batista, S. Marini, N. Chauvin, A. Chancé, D. Uriot, and P. A. P. Nghiem, "Simulations of transverse dynamics in a laser-plasma accelerator", *J. Phys.: Conf. Ser.*, vol. 3094, no. 1, p. 012018, Sep. 2025. doi:10.1088/1742-6596/3094/1/012018